

A. Bakytzy<sup>1</sup>, Z.T. Karipbayev<sup>1\*</sup>, Y. Suchikova<sup>2</sup>, A.B. Usseinov<sup>1</sup>, T.A. Koketai<sup>3</sup>,  
N.K. Mussabek<sup>3</sup>, A.I. Popov<sup>4</sup>

<sup>1</sup>L.N. Gumilyov Eurasian National University, Astana, Kazakhstan;

<sup>2</sup>Berdiansk State Pedagogical University, Ukraine;

<sup>3</sup>Karaganda Buketov University, Kazakhstan;

<sup>4</sup>University of Latvia, Riga, Latvia

(\*Corresponding author's e-mail: karipbayev\_zht\_1@emu.kz)

## Exploration of $\beta$ -Ga<sub>2</sub>O<sub>3</sub> Ceramics Synthesized via Solid-State Method

$\beta$ -Ga<sub>2</sub>O<sub>3</sub> ceramic was synthesized using the solid-state method, a well-established technique for creating ceramic materials with controlled composition and structure. The process began by pressing gallium oxide (Ga<sub>2</sub>O<sub>3</sub>) powder into a unified form, ensuring even distribution and compactness of the material. This pressed form was then subjected to annealing at 1400 °C for 10 hours, a critical step facilitating the formation of a stable and crystalline  $\beta$ -Ga<sub>2</sub>O<sub>3</sub> phase. Energy dispersive X-ray analysis (EDS) was employed to investigate the elemental composition of the synthesized  $\beta$ -Ga<sub>2</sub>O<sub>3</sub> ceramic. The analysis confirmed that the material closely adhered to the ideal stoichiometric ratio of oxygen to gallium (O/Ga) at 3:2, ensuring the purity and consistency of the ceramic. The optical properties of the  $\beta$ -Ga<sub>2</sub>O<sub>3</sub> ceramics were thoroughly studied. Surface morphology analysis and elemental composition measurements were complemented by the recording of photoluminescence excitation and transmission spectra at successive wavelengths ranging from 200 to 800 nm. These spectra provided valuable insights into the material's electronic and optical behavior. Both the synthesized  $\beta$ -Ga<sub>2</sub>O<sub>3</sub> ceramic and commercial  $\beta$ -Ga<sub>2</sub>O<sub>3</sub> crystals exhibited distinct photoluminescence peaks in the blue (~2.7 eV) and ultraviolet (3.3, 3.4, 3.8 eV) spectral ranges.

*Keywords:* synthesis,  $\beta$ -Ga<sub>2</sub>O<sub>3</sub> ceramics, photoluminescence, annealing, stoichiometric ratios, morphology, elemental composition, point defects

### Introduction

Gallium oxide (Ga<sub>2</sub>O<sub>3</sub>) stands out due to its broad bandgap, significant breakdown electric field, and unmatched thermal and chemical robustness [1, 2]. These attributes position it as a premier material for high-power electronic devices, UV LEDs, and gas sensors. Moreover, its resilience to radiation damage, bandgap, and thermal stability hint at its potential in advanced scintillators and phosphors. Its luminescence is enhanced through doping with rare-earth ions or other luminescent agents.

Ga<sub>2</sub>O<sub>3</sub> encompasses five recognized phases:  $\alpha$ ,  $\beta$ ,  $\gamma$ ,  $\delta$ , and  $\epsilon$  [3, 4]. The  $\beta$ -phase garners the most attention, being the most stable and noted for its superb electrical and optical characteristics. Specifically,  $\beta$ -Ga<sub>2</sub>O<sub>3</sub> possesses a vast bandgap of 4.9 eV [5] and an impressive breakdown field, approximately 8 MV/cm [6]. Such attributes hint at its capability to surpass silicon carbide (SiC) and gallium nitride (GaN) in power applications.

Notably,  $\beta$ -Ga<sub>2</sub>O<sub>3</sub> has displayed commendable scintillation properties [7, 8]. It emerges as a prime candidate for several applications, with its broad bandgap reducing self-absorption, thus augmenting light output. Its thermal fortitude and radiation resistance also make it apt for challenging settings. The enhanced photoelectric absorption and Compton scattering properties of  $\beta$ -Ga<sub>2</sub>O<sub>3</sub>, attributed to its high atomic number and density, amplify its scintillation efficacy.

For bulk  $\beta$ -Ga<sub>2</sub>O<sub>3</sub> crystal growth, a slew of techniques is available, including casting [9], EFG [10], Czochralski [11, 12], Bridgman [13], Pulsed laser deposition [14], and hydrothermal methods [15]. The EFG method is lauded for its prowess in yielding sizable, top-tier  $\beta$ -Ga<sub>2</sub>O<sub>3</sub> crystals [16]. However, the final crystal's quality can vary based on temperature, extraction rate, and starting material.

In terms of crafting ceramic Ga<sub>2</sub>O<sub>3</sub>, processes such as solid-state reactions [17], sol-gel techniques [18], and spark plasma sintering [19] can be harnessed. While these avenues facilitate various shapes and dimensions, they sometimes fail to deliver the desired electronic crystallographic purity.

Adding to the methods above, novel research has spotlighted remarkable outcomes in manufacturing refractory ceramics, especially magnesium fluoride (MgF<sub>2</sub>) and yttrium-aluminum-garnet (YAG) ceramics,

using a potent electron beam [20–23]. Such breakthroughs have increased enthusiasm for honing this emergent synthesis technique for refractory substances using an influential electron beam.

Solid-phase synthesis offers significant advantages for producing oxide materials, including high-purity products, simplified purification, and enhanced reaction efficiency. This method is scalable, environmentally friendly, and allows for precise control over stoichiometry, crucial for creating complex oxides with specific properties. Direct combination of metal powders or oxides at high temperatures eliminates the need for solvents, simplifying the synthesis process and reducing environmental impact. Solid-phase synthesis is versatile and capable of producing a wide range of oxides — simple, mixed, and doped — by selecting appropriate precursors and conditions. Its simplicity, scalability, and alignment with green chemistry principles make it an attractive choice for materials science research and industrial applications, ensuring phase-pure oxide materials are essential for catalysis, electronics, and materials science sectors.

### Experimental

The synthesis of  $\beta$ -Ga<sub>2</sub>O<sub>3</sub> ceramics was meticulously carried out employing a solid-state method, utilizing an initial  $\beta$ -Ga<sub>2</sub>O<sub>3</sub> powder that boasted an exceptionally high purity level of 99.999 %. This high-purity powder was methodically pressed into tablets under a substantial pressure of 2 tons, achieving a uniform diameter of 1 cm for each tablet. Figure 1 shows a pressed  $\beta$ -Ga<sub>2</sub>O<sub>3</sub> ceramic. Subsequently, these compacted tablets were subjected to a rigorous annealing process within the confines of a high-temperature furnace. The annealing procedure was conducted for an extended duration of 10 hours, at a significantly high temperature of 1400 °C, ensuring the tablets were placed in an alundum crucible to withstand the high-temperature conditions. Following the annealing phase, the ceramic segments were allowed to gradually return to ambient temperature, a crucial step to prevent thermal shock and ensure structural integrity. Once cooled, these segments were then meticulously segmented and subjected to a thorough analysis to assess their structural and compositional attributes. This careful and precise synthesis process is aimed at achieving optimal ceramic properties through controlled high-temperature treatment and subsequent detailed examination of the resulting ceramic segments.



Figure 1.  $\beta$ -Ga<sub>2</sub>O<sub>3</sub> ceramics

The surface morphology of the crafted ceramic samples was inspected using a Hitachi TM3030 scanning electron microscope, paired with a BrukerXFlash MIN SVE energy dispersive system (or energy-dispersive spectroscopy, EDS), set at an acceleration voltage of 15 kV. This was integral for the compositional analysis of  $\beta$ -Ga<sub>2</sub>O<sub>3</sub>. To further comprehend the ceramics' electronic and optical characteristics, excitation and PL emission spectra were logged in a wavelength span between 200 and 800 nm. These measurements were conducted using a CM-2203 spectrofluorimeter at room temperature. For a more comprehensive interpretation, the data from these newly synthesized samples were juxtaposed with equivalent metrics obtained from commercially available unintentional doped (UID)  $\beta$ -Ga<sub>2</sub>O<sub>3</sub> crystals with *a* (–201) orientation, sourced from Tamura Corp., Japan.

### Results and Discussion

#### *Luminescence spectra of sintered and commercial $\beta$ -Ga<sub>2</sub>O<sub>3</sub> ceramic*

Figure 2(a, b) showcases the photoluminescence spectra of both newly synthesized ceramics and commercial crystals upon excitation at 4.9 eV. Through the application of Gaussian approximation, we were able to delineate three separate components within these spectra. These identified components are characterized by peaks that correspond to blue luminescence, observed at approximately 2.7 eV, and UV luminescence, noted at energy levels of 3.3, 3.4, and 3.8 eV, as illustrated in Figure 2(a). A comparative analysis of the spectra from both the synthesized ceramics and the commercial crystals reveals a striking similarity in their overall profiles. However, a discernible variation is observed in the luminescence peak of the synthesized ceramics, which manifests at a slightly diminished energy level, around 3 eV, as indicated in Figure 2(a). This downward shift in energy suggests the presence of structural distortions and defects within the crystal lattice of the synthesized ceramics. These structural anomalies are implicated in the modification of electronic properties, thereby rendering them distinct from those observed in commercial crystals. The observed reduction in luminescence intensity can be attributed to two primary factors: a decrease in the levels of oxygen vacancies (VO) and the entrapment of electrons, which are essential for luminescence, by specific defect sites or traps within the crystal structure.

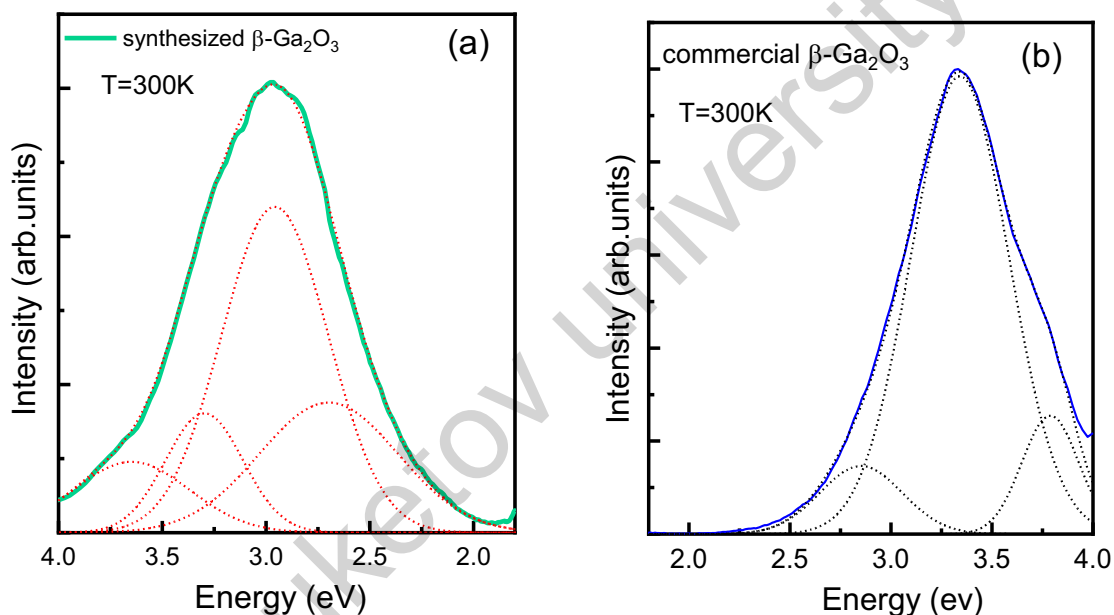


Figure 2.  $\beta$ -Ga<sub>2</sub>O<sub>3</sub> ceramics synthesized under a powerful electron beam

#### *Surface morphology and elemental composition*

The equipment utilized facilitated the examination of three-dimensional samples with shadow and volume contrast, achieving a resolution as precise as 30 nm. As depicted in Figure 3, the standard SEM images of the crafted  $\beta$ -Ga<sub>2</sub>O<sub>3</sub> ceramic surfaces span an area of roughly 0.016 mm<sup>2</sup> (a), and the magnified image of the powdered sample is 1000 times its original size (b). The derived ceramic exhibits a unified surface structure, signifying the total elimination of powder granules or other defects, culminating in a solidified phase. The primary gallium oxide powder comprises particles ranging from 1 to 15  $\mu$ m, as shown in Figure 3b.

The composition of the synthesized  $\beta$ -Ga<sub>2</sub>O<sub>3</sub> ceramic is meticulously aligned with the ideal stoichiometric ratio of oxygen to gallium (O/Ga) of 3/2, a proportion that is critical for achieving desired material properties and is comprehensively documented in Table [24]. This precise compositional alignment mirrors the stoichiometric design principles established in prior studies of  $\beta$ -Ga<sub>2</sub>O<sub>3</sub> nanowires [25, 26], underscoring the reproducibility and precision of the synthesis process. Notably, post-annealing treatments have been observed to significantly alter the O/Ga ratio, leading to a notable reduction in gallium content alongside an increase in oxygen levels. This shift towards a higher oxygen content is attributable to the environmental oxygen influx and the subsequent reduction in vacancy concentrations within the crystal lattice, a phenomenon

consistent with behaviors observed in other crystalline oxide systems [27–38]. Such alterations in stoichiometry highlight the dynamic nature of the material's composition, influenced by thermal treatments. Moreover, the initial stoichiometry of the gallium oxide powder used in the synthesis process closely mirrors that of the annealed ceramic samples, indicating a high fidelity in the transference of stoichiometric ratios from the starting materials to the final ceramic product. This observation reinforces the importance of precise starting material composition for achieving the desired characteristics in the annealed ceramics.

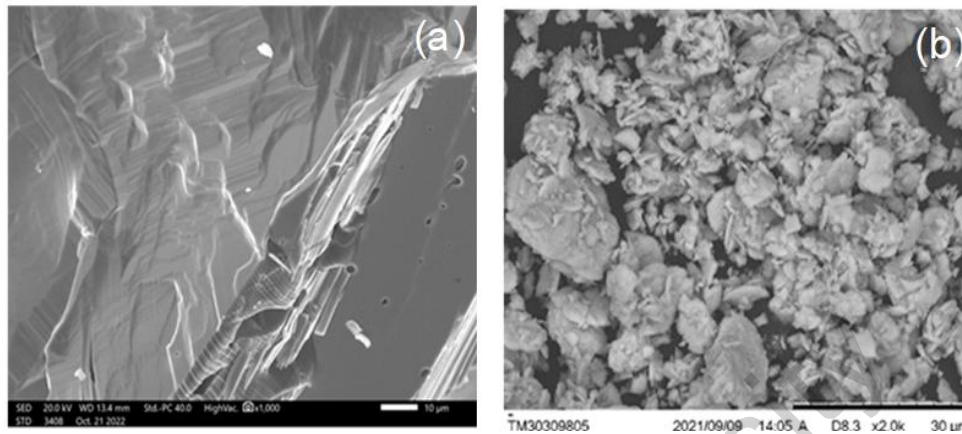


Figure 3. SEM images of synthesized ceramics and the initial  $\text{Ga}_2\text{O}_3$  powder

Table

**Elemental analysis of the powder sample and synthesized  $\beta\text{-Ga}_2\text{O}_3$  ceramics (in At. %)**

| Atom       | Synthesized $\beta\text{-Ga}_2\text{O}_3$ | Pristine powder $\beta\text{-Ga}_2\text{O}_3$ |
|------------|---|---|
| Ga         | 33.2                                      | 33.4  |
| O          | 66.8                                      | 66.6  |
| O/Ga ratio | 2.0                                       | 1.99  |

### Conclusions

The spectral, surface morphology and elemental composition of  $\beta\text{-Ga}_2\text{O}_3$  ceramics derived from a powdered sample under the influence of a potent solid-state synthesis method have been investigated. These attributes were further compared to the properties of commercial crystals utilized in solar-blind photodetector and scintillator manufacturing. The spectral characteristics of the created ceramics closely mirror those of commercial crystals. When excited in the primary absorption band, the variance in luminescence spectra between the crafted ceramics and commercial crystals can be attributed to lingering distortions and flaws. These irregularities are notably diminished after further annealing. Post-annealing, UV luminescence remains a predominant component of the entire spectrum, but blue luminescence diminishes. This reduction is attributed to the partial annealing of oxygen vacancies and the trapping of luminescent electrons by specific sites. Moreover, the annealing process enhances the Ga/O ratio, giving it an edge over commercial crystals.

The solid-state synthesis method paves the way for the more rapid and cost-efficient creation of  $\beta\text{-Ga}_2\text{O}_3$  ceramics, negating the necessity for supplementary equipment or interventions. This method is an effective strategy for generating doped and pure refractory ceramics with elevated melting thresholds.

### Acknowledgment

This research has been funded by the Science Committee of the Ministry of Science and Higher Education of the Republic of Kazakhstan (Grant No. AP14972858). Furthermore, J. Purans is grateful to the ERAF project 1.1.1.1/20/A/057. In addition, the research of A.P. and Y.S. was partly supported by COST Action CA20129 “Multiscale Irradiation and Chemistry Driven Processes and Related Technologies” (MultiChem). J.P. and A.P. thank to the Institute of Solid-State Physics, University of Latvia. ISSP UL as the Center of Excellence is supported through the Framework Program for European universities, Union Horizon 2020, H2020-WIDESPREAD-01–2016–2017-TeamingPhase2, under Grant Agreement No. 739508, CAMART2 project.

## References

- 1 Usseinov, A., Koishybayeva, Z., Platonenko, A., Purans, J., & Popov, A.I. (2021). Vacancy defects in Ga<sub>2</sub>O<sub>3</sub>: First-principles calculations of electronic structure. *Materials*, 14 (23), 7384; <https://doi.org/10.3390/ma14237384>
- 2 Suchikova, Y., Lazarenko, A., Kovachov, S., Karipbaev, Z., & Popov, A.I. (2022). Formation of porous Ga<sub>2</sub>O<sub>3</sub>/GaAs layers for electronic devices. *Proceedings of the 16th International Conference on Advanced Trends in Radioelectronics, Telecommunications and Computer Engineering, TCSET 2022*, 410–413; <https://doi.org/10.1109/TCSET55632.2022.9766890>
- 3 Stepanov, S.I., Nikolaev, V.I., Bougrov, V.E., & Romanov, A.E. (2016). Gallium Oxide: Properties and Applications. *A Review, Rev. Adv. Mater. Sci.*, 44, 63–86.
- 4 Mastro, M.A., Kuramata, A., Calkins, J., Kim, J., Ren, F., & Pearton, S.J. (2017). Perspective — Opportunities and Future Directions for Ga<sub>2</sub>O<sub>3</sub>. *ECS J. Solid State Sci. Technol.*, 6, 356–359; <https://doi.org/10.1149/2.0031707jss>
- 5 Orita, M., Ohta, H., Hirano, M., & Hosono, H. (2000). Deep-Ultraviolet Transparent Conductive  $\beta$ -Ga<sub>2</sub>O<sub>3</sub> Thin Films. *Appl. Phys. Lett.*, 77, 4166–4168 <https://doi.org/10.1063/1.1330559>
- 6 Varley, J.B. & Schleife, A. (2015). Bethe–Salpeter Calculation of Optical-Absorption Spectra of In<sub>2</sub>O<sub>3</sub> and Ga<sub>2</sub>O<sub>3</sub>. *Semicond. Sci. Technol.*, 30, 024010 <https://doi.org/10.1088/0268-1242/30/2/024010>
- 7 Li, W., Zhao, X., Zhi, Y., Zhang, X., Chen, Z., Chu, X., Yang, H., Wu, Z., & Tang, W. (2018). Fabrication of Cerium-Doped  $\beta$ -Ga<sub>2</sub>O<sub>3</sub> Epitaxial Thin Films and Deep Ultraviolet Photodetectors. *Appl. Opt.*, 57, 538; <https://doi.org/10.1364/AO.57.000538>
- 8 Luchechko, A., Vasylytsiv, V., Zhydachevskyy, Y., Kushlyk, M., Ubizskii, S., & Suchocki, A. (2020). Luminescence Spectroscopy of Cr<sup>3+</sup> Ions in Bulk Single Crystalline  $\beta$ -Ga<sub>2</sub>O<sub>3</sub>. *J. Phys. D. Appl. Phys.*, 53, 354001; <https://doi.org/10.1088/1361-6463/ab8c7d>
- 9 Xia, N., Liu, Y., Wu, D., Li, L., Ma, K., Wang, J., Zhang, H., & Yang, D. (2023).  $\beta$ -Ga<sub>2</sub>O<sub>3</sub> Bulk Single Crystals Grown by a Casting Method. *J. Alloys Compd.*, 935, 168036; <https://doi.org/10.1016/j.jallcom.2022.168036>
- 10 Aida, H., Nishiguchi, K., Takeda, H., Aota, N., Sunakawa, K., & Yaguchi, Y. (2008). Growth of  $\beta$ -Ga<sub>2</sub>O<sub>3</sub> Single Crystals by the Edge-Defined, Film Fed Growth Method. *Jpn. J. Appl. Phys.*, 47, 8506–8509; <https://doi.org/10.1143/JJAP.47.8506>
- 11 Galazka, Z., Uecker, R., Irmscher, K., Albrecht, M., Klimm, D., Pietsch, M., Brützm, M., Bertram, R., Ganschow, S., & Fornari, R. (2010). Growth and Characterization of  $\beta$ -Ga<sub>2</sub>O<sub>3</sub> Single Crystals. *Cryst. Res. Technol.*, 45, 1229–1236 <https://doi.org/10.1002/crat.201000341>
- 12 Tamm, Y., Reiche, P., Klimm, D., & Fukuda, T. (2000). Czochralski grown Ga<sub>2</sub>O<sub>3</sub> crystals. *J. Cryst. Growth* 220, 510–514; [https://doi.org/10.1016/S0022-0248\(00\)00851-4](https://doi.org/10.1016/S0022-0248(00)00851-4)
- 13 Galazka, Z. (2022). Growth of Bulk  $\beta$ -Ga<sub>2</sub>O<sub>3</sub> Single Crystals by the Czochralski Method. *J. Appl. Phys.*, 131, 031103; <https://doi.org/10.1063/5.0076962>
- 14 Hoshikawa, K., Ohba, E., Kobayashi, T., Yanagisawa, J., Miyagawa, C., & Nakamura, Y. (2016). Growth of  $\beta$ -Ga<sub>2</sub>O<sub>3</sub> Single Crystals Using Vertical Bridgman Method in Ambient Air. *J. Cryst. Growth*, 447, 36–41; <https://doi.org/10.1016/j.jcrysgro.2016.04.022>
- 15 Wakabayashi, R., Oshima, T., Hattori, M., Sasaki, K., Masui, T., Kuramata, A., Yamakoshi, S., Yoshimatsu, K., & Ohtomo, A. (2015). Oxygen-Radical-Assisted Pulsed-Laser Deposition of  $\beta$ -Ga<sub>2</sub>O<sub>3</sub> and  $\beta$ -(Al<sub>x</sub>Ga<sub>1-x</sub>)<sub>2</sub>O<sub>3</sub> Films. *J. Cryst. Growth*, 424, 77–79; <https://doi.org/10.1016/j.jcrysgro.2015.05.005>
- 16 Kang, B.K., Mang, S.R., Lim, H.D., Song, K.M., Song, Y.H., Go, D.H., Jung, M.K., Senthil, K., & Yoon, D.H. (2014). Synthesis, Morphology and Optical Properties of Pure and Eu<sup>3+</sup> Doped  $\beta$ -Ga<sub>2</sub>O<sub>3</sub> Hollow Nanostructures by Hydrothermal Method. *Mater. Chem. Phys.*, 147, 178–183; <https://doi.org/10.1016/j.matchemphys.2014.04.025>
- 17 Fu, B., Mu, W., Li, Y., Shi, Y., Li, Y., Jia, Z., & Tao, X. (2021). Investigation of the Blue Color Center in  $\beta$ -Ga<sub>2</sub>O<sub>3</sub> Crystals by the EFG Method. *Cryst. Eng. Comm.*, 23, 8360–8366. <https://doi.org/10.1039/D1CE101078F>
- 18 Ramana, C.V., Roy, S., Zade, V., Battu, A.K., Makeswaran, N., & Shutthanandan, V. (2021). Electronic Structure and Chemical Bonding in Transition-Metal-Mixed Gallium Oxide (Ga<sub>2</sub>O<sub>3</sub>) Compounds. *J. Phys. Chem. Solids*, 157, 110174. <https://doi.org/10.1016/j.jpcs.2021.110174>
- 19 Gopal, R., Goyal, A., Saini, A., Nagar, M., Sharma, N., Gupta, D.K., & Dhayal, V. (2018). Sol-Gel Synthesis of Ga<sub>2</sub>O<sub>3</sub> Nanorods and Effect of Precursor Chemistry on Their Structural and Morphological Properties. *Ceram. Int.*, 44, 19099–19105. <https://doi.org/10.1016/j.ceramint.2018.07.173>
- 20 Yu, S., Zhang, G., Carloni, D., & Wu, Y. (2020). Fabrication, Microstructure and Optical Properties of Ga<sub>2</sub>O<sub>3</sub> Transparent Ceramics. *Ceram. Int.*, 46, 21757–21761; <https://doi.org/10.1016/j.ceramint.2020.05.285>
- 21 Alypssova, G., Lisitsyn, V., Golkovski, M., Mussakhanov, D., Karipbayev, Z., Grechkina, T., Karabekova, D. & Kozlovskiy, A. (2021). Luminescence Efficiency of Cerium-Doped Yttrium Aluminum Garnet Ceramics Formed by Radiation Assisted Synthesis. *Eastern-European J. Enterp. Technol.*, 6, 49–57; <https://doi.org/10.15587/1729-4061.2021.246379>
- 22 Karipbayev, Z.T., Lisitsyn, V.M., Mussakhanov, D.A., Alypssova, G.K., Popov, A.I., Polisadova, E.F., Elsts, E., Akilbekov, A.T., Kukenova, A.B., Kemere, M. et al. (2020). Time-Resolved Luminescence of YAG:Ce and YAGG:Ce Ceramics Prepared by Electron Beam Assisted Synthesis. *Nucl. Instruments Methods Phys. Res. Sect. B Beam Interact. with Mater. Atoms*, 479, 222–228; <https://doi.org/10.1016/j.nimb.2020.06.046>
- 23 Lisitsyna, L.A., Popov, A.I., Karipbayev, Z.T., Mussakhanov, D.A., & Feldbach, E. (2022). Luminescence of MgF<sub>2</sub>-WO<sub>3</sub> Ceramics Synthesized in the Flux of 1.5 MeV Electron Beam. *Opt. Mater. (Amst)*, 133, 112999. <https://doi.org/10.1016/j.optmat.2022.112999>

- 24 Avilov, M., Fadeev, S., Fernandes, S., Golkovsky, M., Mittig, W., Pellemoine, F., & Schein, M. (2015). A 50-KW Prototype of the High-Power Production Target for the FRIB. *J. Radioanal. Nucl. Chem.*, 305, 817–823. <https://doi.org/10.1007/s10967-014-3908-1>
- 25 Ahman, J., Svensson, G., & Albertsson, J. (1996). A Reinvestigation of  $\beta$ -Gallium Oxide. *Acta Crystallogr. Sect. C*, 52, 1336–1338. <https://doi.org/10.1107/S0108270195016404>
- 26 Cui, H., Sai, Q., Qi, H., Zhao, J., Si, J., & Pan, M. (2019). Analysis on the Electronic Trap of  $\beta$ -Ga<sub>2</sub>O<sub>3</sub> Single Crystal. *J. Mater. Sci.*, 54, 12643–12649. <https://doi.org/10.1007/s10853-019-03777-1>
- 27 Suchikova, Y., Kovachov, S., Bohdanov, I., Pankratov, V., & Popov, A.I. (2023). Study of the structural and morphological characteristics of the Cd<sub>x</sub>Te<sub>y</sub>O<sub>z</sub> nanocomposite obtained on the surface of the CdS/ZnO heterostructure by the SILAR method. *Appl. Phys. A: Mater. Sci. Process.*, 129, 7, 499; <https://doi.org/10.1007/s00339-023-06776-x>
- 28 Suchikova, Y., Kovachov, S., Bohdanov, I., Moskina, A., & Popov, A. (2023). Characterization of Cd<sub>x</sub>Te<sub>y</sub>O<sub>z</sub>/CdS/ZnO Heterostructures Synthesized by the SILAR Method. *Coatings*, 13 (3), 639. <https://doi.org/10.3390/coatings13030639>
- 29 Vambol, S.O., Bohdanov, I.T., Vambol, V.V., Nestorenko, T.P., & Onyschenko, S.V. (2017). Formation of filamentary structures of oxide on the surface of monocrystalline gallium arsenide. *J. Nano-Electron. Phys.*, 9(6), 06016. [https://doi.org/10.21272/jnep.9\(6\).06016](https://doi.org/10.21272/jnep.9(6).06016)
- 30 Suchikova, Y., Kovachov, S., & Bohdanov, I. (2022). Formation of oxide crystallites on the porous GaAs surface by electrochemical deposition. *Nanometer. Nanotechnol.*, 12. <https://doi.org/10.1177/18479804221127307>
- 31 Kovachov, S., Bohdanov, I., Karipbayev, Z., Tsebriienko, T., & Popov, A.I. (2022). Layer-by-Layer Synthesis and Analysis of the Phase Composition of Cd<sub>x</sub>Te<sub>y</sub>O<sub>z</sub>/CdS/por-ZnO/ZnO Heterostructure. *Proc. 2022 IEEE 3rd KhPI Week on Adv. Technol., KhPI Week 2022*. <https://doi.org/10.1109/KhPIWeek57572.2022.9916492>
- 32 Usseinov, A., Platonenko, A., Koishybayeva, Z., Akilbekov, A., Zdorovets, M., & Popov, A.I. (2022). Pair vacancy defects in  $\beta$ -Ga<sub>2</sub>O<sub>3</sub> crystal: Ab initio study. *Optical Materials: X*, 16, 100200. <https://doi.org/10.1016/j.omx.2022.100200>
- 33 Zachinskis, A., Grechenkov, J., Butanovs, E., Platonenko, A., Piskunov, S., Popov, A.I., Purans, J., & Bocharov, D. (2023). Ir impurities in  $\alpha$ - and  $\beta$ -Ga<sub>2</sub>O<sub>3</sub> and their detrimental effect on p-type conductivity. *Scientific Reports*, 13(1), 8522. <https://doi.org/10.1038/s41598-023-35112-9>
- 34 Usseinov, A., Koishybayeva, Z., Platonenko, A., Akilbekov, A., Purans, J., Pankratov, V., Suchikova, Y., & Popov, A.I. (2021). Ab-Initio Calculations of Oxygen Vacancy in Ga<sub>2</sub>O<sub>3</sub> Crystals. *Latv. J. Phys. Tech. Sci.*, 58, 3–10. <https://doi.org/10.2478/lpts-2021-0007>
- 35 Klym, H., Karbovnyk, I., Luchechko, A., Kostiv, Y., Pankratova, V., & Popov, A.I. (2021). Evolution of Free Volumes in Polycrystalline BaGa<sub>2</sub>O<sub>4</sub> Ceramics Doped with Eu<sup>3+</sup> Ions. *Crystals*, 11, 1515. <https://doi.org/10.3390/cryst11121515>
- 36 Luchechko, A., Zhdachevskyy, Y., Ubizskii, S., Kravets, O., Popov, A.I., Rogulis, U., Elsts, E., Bulur, E., & Suchocki, A. (2019). Afterglow, TL and OSL Properties of Mn<sup>2+</sup>-doped ZnGa<sub>2</sub>O<sub>4</sub> Phosphor. *Scientific Reports Rep.*, 9, 9544. <https://doi.org/10.1038/s41598-019-45869-7>
- 37 Klym, H., Karbovnyk, I., Luchechko, A., Kostiv, Y., & Popov, A.I. (2022). Extended positron trapping defects in the Eu<sup>3+</sup>-doped BaGa<sub>2</sub>O<sub>4</sub> ceramics studied by PAL method. *Phys. Status Solidi*, 259, Article 2100485, 10.1002/pssb.202100485
- 38 Luchechko, A., Zhdachevskyy, Y., Sugak, D., Kravets, O., Martynyuk, N., Popov, A.I., Ubizskii, S., & Suchocki, A. (2019). Luminescence Properties and Decay Kinetics of Mn<sup>2+</sup> and Eu<sup>3+</sup> Co-Dopant Ions in MgGa<sub>2</sub>O<sub>4</sub> Ceramics. *Latv. J. Phys. Tech. Sci.*, 55, 43–51. <https://doi.org/10.2478/lpts-2018-0043>

А. БАҚЫТҚЫЗЫ, Ж.Т. ҚАРИПБАЕВ, Я. СУЧИКОВА, А.Б. УСЕЙНОВ,  
Т.Ә. КӨКЕТАЙ, Н.Қ. МҰСАБЕК, А.И. ПОПОВ

## Қатты дене әдісімен синтезделген $\beta$ -Ga<sub>2</sub>O<sub>3</sub> керамикасын зерттеу

$\beta$ -Ga<sub>2</sub>O<sub>3</sub> керамикалық құрамы мен құрылымы бақыланатын керамикалық материалдарды жасаудың жақсы қалыптасқан әдісі қатты күй әдісі арқылы синтездеу. Процесс материалдың біркелкі таралуы мен ықшамдылығын қамтамасыз ететін галлий оксиді (Ga<sub>2</sub>O<sub>3</sub>) ұнтағын біртұтас пішінге престеу арқылы басталады. Содан кейін бұл престелген пішін 1400 °C температурада 10 сағат бойы жасытуға ұшырайды, бұл тұрақты және кристалды  $\beta$ -Ga<sub>2</sub>O<sub>3</sub> фазасының түзілуін жеңілдететін маңызды қадам. Синтезделген  $\beta$ -Ga<sub>2</sub>O<sub>3</sub> керамикасының элементтік құрамын зерттеу үшін энергетикалық дисперсиялық рентгендік талдау (EDS) қолданылды. Талдау материалдың керамиканың тазалығы мен консистенциясын қамтамасыз ете отырып, оттегі мен галлийдің (O/Ga) мінсіз стехиометриялық арақатынасына 3:2 сәйкес келетінін растады.  $\beta$ -Ga<sub>2</sub>O<sub>3</sub> керамикасының оптикалық қасиеттері мұқият зерттелді. Беттік морфологияны талдау және элементтік құрамды өлшеу 200-ден 800 нм-ге дейінгі дәйекті толқын ұзындығында фотолюминесценцияның козуы мен өткізу спектрлерін тіркеумен толықтырылды. Бұл спектрлер материалдың электрондық және оптикалық қасиеттері туралы құнды түсініктер береді. Синтезделген  $\beta$ -Ga<sub>2</sub>O<sub>3</sub> керамикалық және коммерциялық  $\beta$ -Ga<sub>2</sub>O<sub>3</sub> кристалдары көк (~2,7 эВ) және ультракүлгін (3,3, 3,4, 3,8 эВ) спектрлік диапазондарда фотолюминесценцияның айқын шыңдарын көрсетті.

*Кілт сөздер:* синтез,  $\beta$ -Ga<sub>2</sub>O<sub>3</sub> керамика, фотолюминесценция, күйдіру, стехиометриялық қатынас, морфология, элементтік құрам, нүктелік ақаулар

А. Бакыткызы, Ж.Т. Карипбаев, Я. Сучикова, А.Б. Усеинов,  
 Т.А. Кокетай, Н.К. Мусабек, А.И. Попов

## Исследование керамики $\beta$ -Ga<sub>2</sub>O<sub>3</sub>, синтезированной твердотельным методом

Керамика  $\beta$ -Ga<sub>2</sub>O<sub>3</sub> была синтезирована с использованием твердотельного метода, хорошо зарекомендовавшего себя в создании керамических материалов с контролируемым составом и структурой. Процесс начался с прессования порошка оксида галлия (Ga<sub>2</sub>O<sub>3</sub>) в единую форму, что обеспечило равномерное распределение и компактность материала. Затем прессованная форма была подвергнута отжигу при 1400 С в течение 10 часов, что является важным шагом, способствующим образованию стабильной и кристаллической фазы  $\beta$ -Ga<sub>2</sub>O<sub>3</sub>. Для исследования элементного состава синтезированной керамики  $\beta$ -Ga<sub>2</sub>O<sub>3</sub> был использован энергодисперсионный рентгеновский анализ (EDS), который подтвердил, что материал близок к идеальному стехиометрическому соотношению кислорода к галлию (O/Ga) в 3:2, что обеспечивает чистоту и однородность керамики. Оптические свойства керамики  $\beta$ -Ga<sub>2</sub>O<sub>3</sub> были тщательно изучены. Анализ морфологии поверхности и измерения элементного состава были дополнены регистрацией спектров возбуждения и пропускания фотолюминесценции на последовательных длинах волн в диапазоне от 200 до 800 нм. Эти спектры предоставили ценную информацию об электронных и оптических свойствах материала. Как синтезированная керамика  $\beta$ -Ga<sub>2</sub>O<sub>3</sub>, так и коммерческие кристаллы  $\beta$ -Ga<sub>2</sub>O<sub>3</sub> показали отчетливые пики фотолюминесценции в синем (~2,7 эВ) и ультрафиолетовом (3,3, 3,4, 3,8 эВ) спектральных диапазонах.

*Ключевые слова:* синтез, керамика  $\beta$ -Ga<sub>2</sub>O<sub>3</sub>, фотолюминесценция, отжиг, стехиометрические соотношения, морфология, элементный состав, точечные дефекты

### Information about the authors

**Bakytkyzy, Aizat** — PhD student, Institute of Physical and Technical Sciences, L.N. Gumilyov Eurasian National University, Astana 010008, Kazakhstan; e-mail: [kukenova\\_ab\\_1@enu.kz](mailto:kukenova_ab_1@enu.kz); ORCID ID: <https://orcid.org/0000-0002-6304-8365>

**Karipbayev, Zhakyp** (*corresponding author*) — PhD, Institute of Physical and Technical Sciences, L.N. Gumilyov Eurasian National University, Astana 010008, Kazakhstan; e-mail: [karipbayev\\_zht\\_1@enu.kz](mailto:karipbayev_zht_1@enu.kz); ORCID ID: <https://orcid.org/0000-0003-4066-1826>

**Suchikova, Yana** — Doctor of physical and mathematical sciences, Professor of the Department of Physics and Methods of Teaching Physics, Berdyansk State Pedagogical University, 71100 Berdyansk, Ukraine; e-mail: [yanasuchikova@gmail.com](mailto:yanasuchikova@gmail.com); ORCID ID: <https://orcid.org/0000-0003-4537-966X>

**Usseinov, Abay** — PhD, Institute of Physical and Technical Sciences, L.N. Gumilyov Eurasian National University, Astana 010008, Kazakhstan; e-mail: [usseinov\\_ab@enu.kz](mailto:usseinov_ab@enu.kz); ORCID ID: <https://orcid.org/0000-0002-4066-8422>

**Koketay, Temirgali** — Doctor of physical and mathematical sciences, Professor, Department of Physics and Nanotechnology, Karaganda Buketov University, Karaganda, Kazakhstan; e-mail: [katkargu@mail.ru](mailto:katkargu@mail.ru); <https://orcid.org/0000-0003-2575-7280>

**Mussabek, Nurassyl** — Master of Science, Institute of Technical Physics and Ecological Problems, Karaganda Buketov University, Karaganda, Kazakhstan; e-mail: [nyri-t-ara@mail.ru](mailto:nyri-t-ara@mail.ru); ORCID ID: <https://orcid.org/0009-0002-4319-3319>

**Popov, Anatoli** — Doctor of physical and mathematical sciences, Professor, Institute of Solid-State Physics, University of Latvia, 8 Kengaraga Str., Lv-1063 Riga, Latvia; e-mail: [popov@latnet.lv](mailto:popov@latnet.lv); ORCID ID: <https://orcid.org/0000-0003-2795-9361>